1. INTRODUCTION

1.1. III-Nitride Materials and Devices in Power Electronics

In the past decade, wide-bandgap nitride semiconductor materials have attracted increasing attention for high-power and high-temperature electronic devices. Due to the strong polarity of the III-nitride bond, the III-nitrides exhibit remarkable chemical, physical and thermal properties. Furthermore, III-nitride materials possess some unique advantages, such as wide bandgap, high electron saturation drift velocity, high electric field strength, high thermal conductivity, and the possibility of lattice-matched heterostructure formation.[1] All of these properties are crucial for the realization of recently emerging power electronic devices, which are required to operate at higher power levels, and in high-temperature and hostile environments.

There are many types of power electronic devices ranging from Schottky diodes, *p-i-n* diodes, heterostructure field effect transistors (HFETs), heterostructure bipolar transistors (HBTs), and thyristors that can be used to realize the power supply function of rectifying and switching. However, simple device structures, such as Schottky rectifiers and *p-i-n* rectifiers, are the most immediate means to exploit the superior properties and high-power handling capability of III-nitride materials. In addition, the study of these basic devices allows us to obtain the fundamental material properties and to further explore the potential applications of more complicated devices. In this program, carried out a Georgia Tech, the characteristics of GaN *p-i-n* rectifiers grown on SiC and GaN substrates were studied. We have demonstrated excellent performance of high-voltage characteristics combined with low on-resistance for GaN *p-i-n* rectifiers grown on SiC and "bulk" GaN substrates.

1.2 Advantage of III-Nitride *p-i-n* Rectifiers

The primary advantage of employing *p-i-n* rectifiers as power devices is to benefit from the low resistance during the "On-state" operation and high breakdown voltage. Thus, the device can sustain a high current density under forward bias with low power losses [2,3] - one of the main critical aspects for many high-power device applications.

To realize the high-performance and reliable nitride power rectifiers, the nitride material quality plays an indispensable role. Currently, the lack of a convenient large-area lattice-matched substrate creates many problems in the epitaxial growth of quality III-nitride films. Most of the epitaxial growth of nitride films has been performed on basal plane (*c*-plane) sapphire substrates (α-Al_2O_3) because it has hexagonal wurtzite crystal structure same as thermodynamically stable structure of GaN; is inexpensive; and has a high thermal stability. However, there is a 10% lattice mismatch between the III-nitride epitaxial layer and the sapphire substrates. In this research program, the development of GaN *p-i-n* rectifier structure grown on lattice-less-mismatched (SiC) or lattice-matched (GaN) and thermally compatible substrate materials was performed to greatly improve the device performance characteristics. The research activities include new device structure design, the epitaxial growth by metalorganic chemical vapor deposition, device fabrication, and characterization of the devices.

2. TECHNICAL APPROACH FOR THE DEVELOPMENT OF NITRIDE *P-I-N* RECTIFIERS

2.1. Growth and Material Characterization of Rectifier Structures

2.1.1. Epitaxial materials growth by MOCVD and material characterization

GaN epitaxial materials used in this study were grown on *n*-type SiC and GaN substrates by metalorganic chemical vapor deposition (MOCVD) using a Thomas Swan Scientific reactor system equipped with close-coupled showerhead (CCS) growth technology [4]. Ultra-pure hydrogen (H_2) was used as the carrier gas mixed with ammonia (NH_3) as hydride precursor and with EpiPure^{TM}[5] trimethylgallium (TMGa) as alkyl precursors. Silane (SiH_4) and bis-cyclopentadienyl magnesium (Cp_2Mg) were used as *n*- and *p*-type dopant precursors, respectively. Prior to the epitaxial growth, the crystalline quality and the surface morphology (both macroscopically and microscopically) of the SiC and GaN substrates were characterized by X-ray diffraction (XRD), polariscope, Nomarski optical microscope, and atomic-force microscopy (AFM). The substrates underwent the solvent cleaning as well as a dip in dilute hydrofluoric acid before epitaxial growth. The substrates were also cleaned in the reactor chamber in-situ using a five-minute, high-temperature bake-out in a H_2 ambient.

Material characterization of the epitaxial structures after growth was performed. Examination with Nomarski optical microscope and AFM were employed for macroscopic and microscopic surface morphology investigation. The crystalline quality of GaN epitaxial layers was analyzed using a high-resolution XRD. The free carrier concentrations and mobilities in the *p*-type and *n*-type GaN for the rectifier structure were determined by 300K Hall-effect measurements. Photoluminescence was also used for optical characterization of the materials grown.

2.1.2. GaN buffer layer development on SiC substrates

Dupuis' lab move to Georgia Tech resulted in the purchase and installation of two new III-nitride MOCVD systems; new growth condition calibration and optimization for rectifier structure using new tools were required. We have achieved high-quality GaN growth on sapphire and SiC substrates. GaN-based epitaxial structures can be grown on sapphire substrates, SiC substrates, or GaN substrates. We grew *p-i-n* rectifier structure on different substrates to study the effect of substrates on *p-i-n* rectifier having nominally the same structure in terms of breakdown voltage, forward turn-on voltage, and on-state resistance. The rectifier performance characteristics in relation to material/crystalline qualities were studied by comparing the structures grown on different substrates. We have found that GaN layers grown on SiC substrates generally have better crystalline quality than one grown on sapphire substrate. (See Figure 1).

We obtained excellent crystalline quality of GaN layers, which will be used for buffer layer of the rectifier structures, having narrow line width of X-ray diffraction peak from symmetric and asymmetric X-ray rocking curve scans Figure 1 shows symmetric and asymmetric X-ray rocking curves for a ~2μm-thick GaN layer grown on a SiC substrate. Linewidth of the peaks exhibit full-width-at-half-maximum (FWHM) values of ~230 and ~280 arc-s. for (002) and (102) diffraction conditions, respectively. Rocking curve peaks from GaN on SiC (<300 arc-s. for (102) scan) are generally narrower than ones on sapphire substrate (>400 arc-s. for (102) scan, in general), supporting better crystalline quality of the layer on SiC

substrates. The FWHM of one of the best ~2-μm thick GaN layers grown on SiC substrates were 150 (002 symmetric reflection) and 270 (102 asymmetric reflection) arc-s.

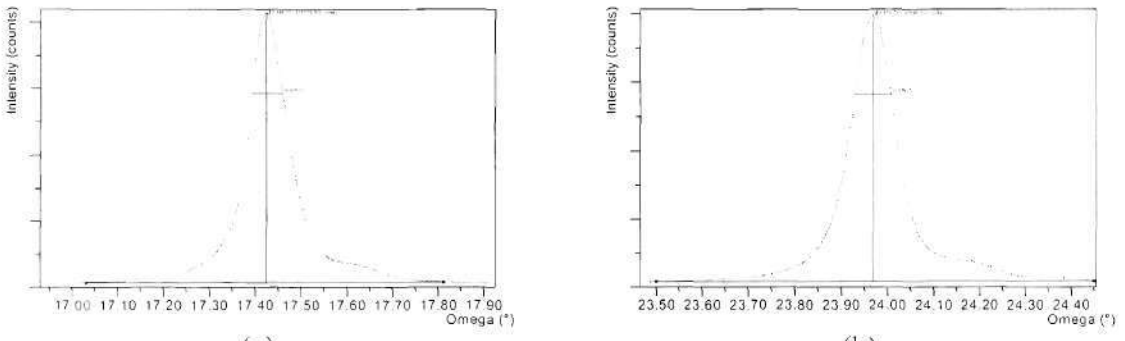

(a) (b)

Figure 1: X-ray rocking curve for 2μm GaN buffer grown on SiC substrate at 300Torr, (a) (002) reflection and (b) (102) reflection.

2.1.3. Calibration for *n*-type GaN:Si and *p*-type GaN:Mg growth conditions

We calibrated growth conditions for GaN:Si layers with *n*-type doping levels ranging from mid-10^{17} to low-10^{20} cm^{-3}, verifying dopant input ratio vs. doping level relation is linear. We studied the *n*-type doping level of GaN layers that will be employed in *p-i-n* rectifier structures. Figure 2 shows the sheet resistance mapping result of the sample, exhibiting ~2.5% resistance uniformity. For the sample shown in Figure 2, the free-electron carrier concentration, *n* was 2×10^{18} cm^{-3} with electron mobility, μ_e~299 cm^2/Vs, as characterized by Hall measurements performed at 300K.

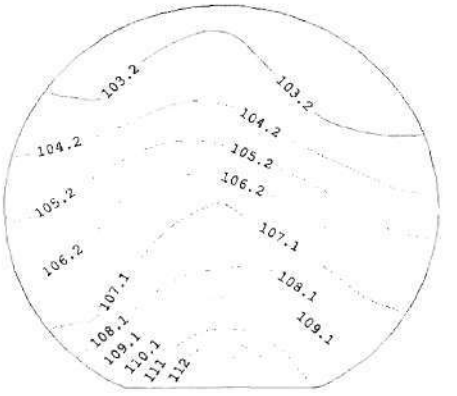

Figure 2: Sheet resistance mapping of *n*-type GaN:Si layer.

For Mg-doped *p*-type GaN layers, we optimized our growth conditions for *p*-type doping to achieve a 300K free-hole concentration of p~$1\times10^{18}cm^{-3}$ with mobility of 13 cm^2/V-s, as determined by the Hall measurements. Variable-temperature Hall data of a typical GaN:Mg layer shows that, as expected, the free-carrier concentration changes as a function of inverse temperature. From the gradient of the 1000/T vs. free-hole concentration plot, an acceptor activation energy of ~170 meV is obtained, which is close to the value reported for the Mg

acceptor in GaN:Mg *p*-type layers. Figure 3 shows the secondary ion mass spectroscopy (SIMS) depth profiling data for a GaN:Mg sample exhibiting a 300K free-hole concentration, $p \sim 1 \times 10^{18}$ cm^{-3}. Unintentional carbon and oxygen impurity levels are well controlled (very low or near the detection limit) and Mg concentration in the GaN layer is [Mg] = 4×10^{19} cm^{-3}, indicating that ~2.5% of Mg incorporated into GaN is activated as a *p*-type dopant.

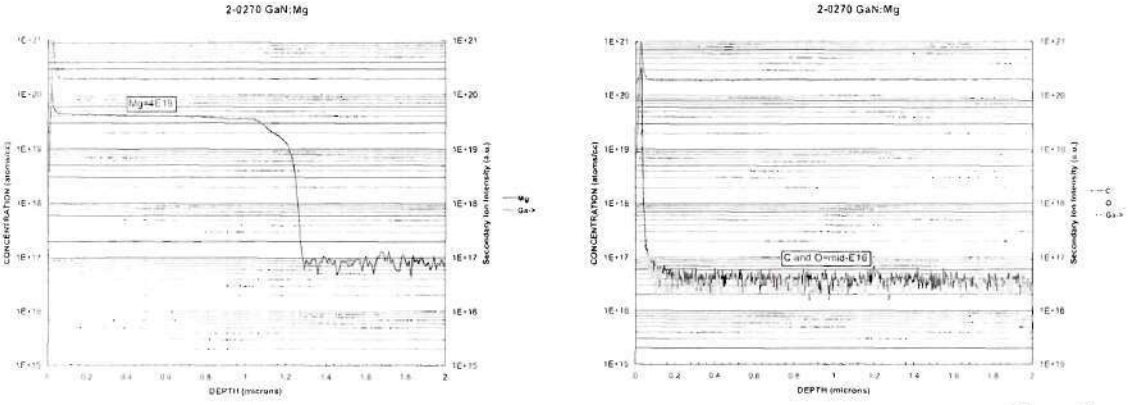

Figure 3: SIMS profile of GaN:Mg layer having free hole concentration, $p \sim 1 \times 10^{18}$ cm^{-3} with 13 cm^2/V-s.

2.2. Rectifier Structure Growth, Fabrication, and Testing

2.2.1. Device fabrication and testing of rectifier structures

Photolithography and inductively-coupled plasma (ICP) etching with Cl_2 and He etching species were employed to define the mesa structure. Then, a wet-chemical cleaning step was used to remove the dry etch damage. Immediately after the wet-cleaning step, an SiO_2 passivation layer was deposited by plasma-enhanced chemical vapor deposition (PECVD). An electron-beam evaporator was used to deposit the *n*-type Ohmic contacts consisting of Ti/Al/Ti/Au (200/700/200/700 Å), and the *p*-type Ohmic contacts of Pd/Au (200/1000 Å). Devices having a mesa diameter of 80 μm with metal contact diameter of 60 μm were fabricated and tested. The current density is based on the mesa area.

The forward *I-V* characteristics and low reverse bias voltage (up to –100V) *I-V* characteristics were measured using a Agilent 4156C precision semiconductor parameter analyzer. The high-voltage reverse *I-V* characteristics (beyond -100V) were measured using a high-voltage test system, which consists of a high-voltage power supply (Stanford Research Systems PS350) and a HP 4142B Modular *I-V* analyzer. ICS Metrics software was used to control the hardware.

2.2.2. Growth of device structure and process flow

A typical structure and SEM image of a GaN *p-i-n* rectifier device grown on SiC substrate is illustrated in Figure 4, while that for *p-i-n* rectifier on GaN substrate is shown in Figure 5. The SEM images clearly show a smooth etched surface, indicating a low-damage etch of the surface. The carrier concentrations for the *p*-type and *n*-type regions were calibrated to be $p \sim 1 \times 10^{18}$ and $n \sim 5 \times 10^{18}$ cm^{-3} from 300K Hall-effect measurements on thicker layers grown under same growth conditions. The carrier concentration of *i*-layer is estimated to be $n \sim 5 \times 10^{16}$ cm^{-3}.

The GaN:Mg^{++} cap layer at the top of the structure was grown for the purpose of achieving Ohmic contacts as well as improving the forward voltage. The growth conditions were optimized for material quality and high carrier concentration in the *p*-type region. In order to minimize the dislocation density of the devices, we have grown GaN *p-i-n* diodes on low-dislocation density (~<1×10^8 cm^{-2}) *n*-type bulk GaN substrates [6].

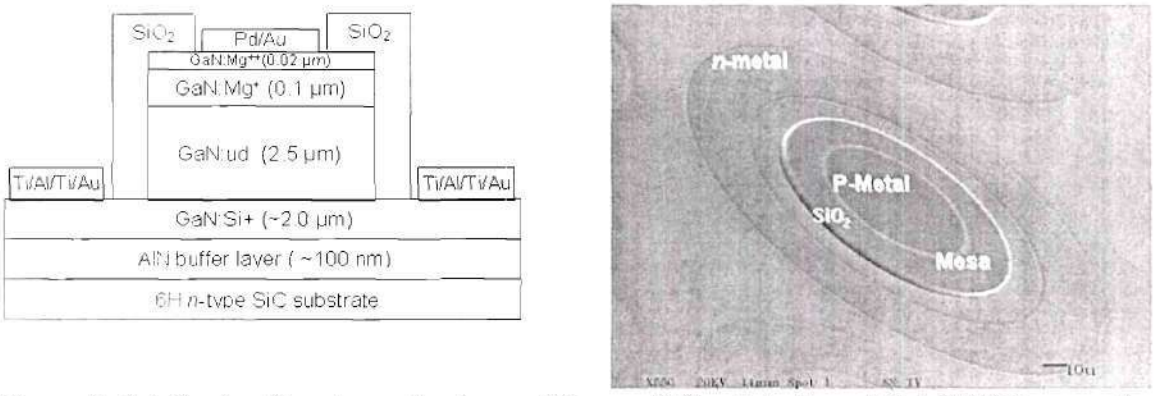

Figure 4: (a) Device Structure of *p-i-n* rectifier on SiC substrate and (b) SEM image of *p-i-n* rectifier on SiC substrate.

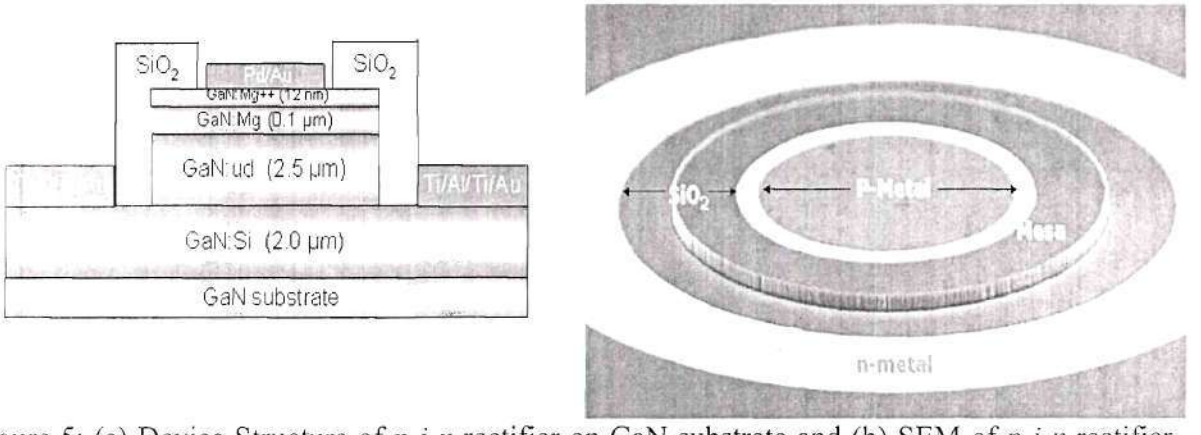

Figure 5: (a) Device Structure of *p-i-n* rectifier on GaN substrate and (b) SEM of *p-i-n* rectifier on GaN substrate.

3. Results and Discussion

3.1. GaN *p-i-n* Mesa Type Rectifiers

3.1.1. Performance characteristics of mesa type rectifiers on SiC substrates

Figure 6(a) shows the high-voltage reverse characteristics for rectifiers grown on a SiC substrate. The reverse current density is I_r ~ 1 A/cm^2 with a blocking voltage of V_r ~ -500 V. The forward *I-V* characteristics are shown in Figure 6(b). The forward voltage drop is ~4.6 V at a typical forward current density of 100 A/cm^2, with the maximum current density exceeding 1900 A/cm^2. The specific On-resistance is R_{ON} ~2.3 mΩ·cm^2. These values yield a figure-of-merit value for $(V_{RB})^2/R_{ON}$ = 108 MW/cm^2.

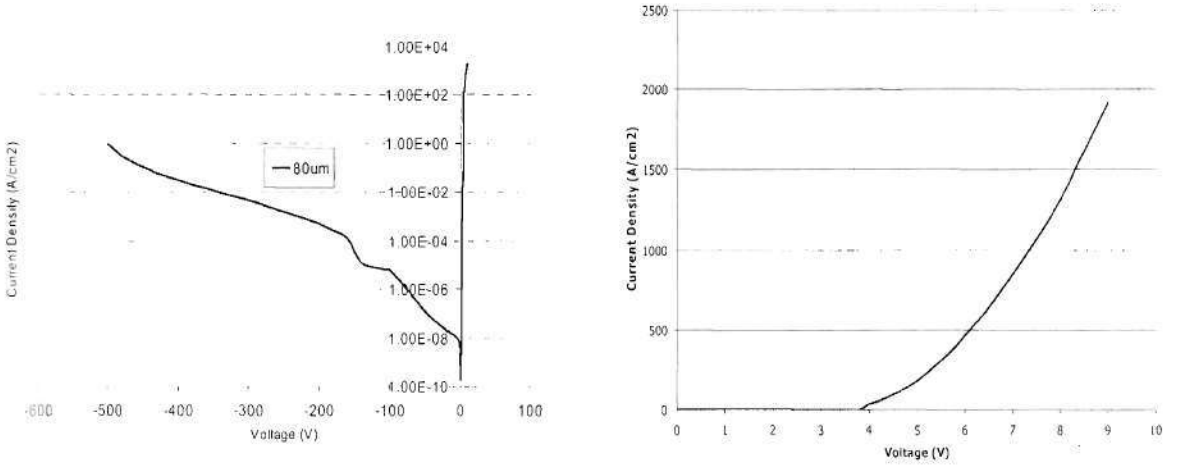

Figure 6: *I-V* characteristics of *p-i-n* rectifier on SiC substrate and (b) forward characteristics of *p-i-n* rectifier on SiC substrate.

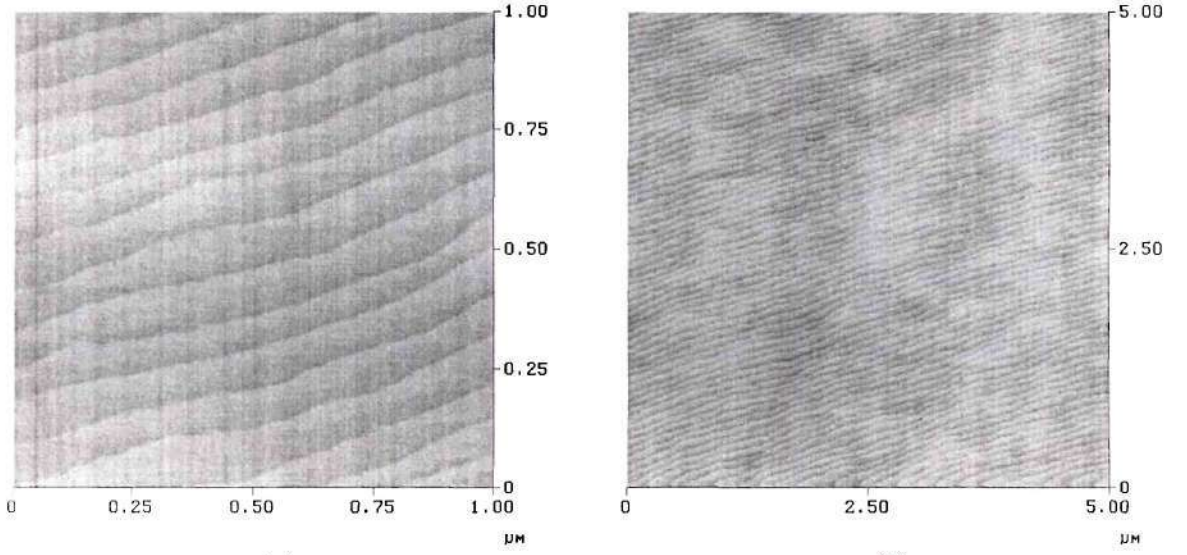

(a) (b)

Figure 7: AFM microscopic surface morphology of a GaN *p-i-n* rectifier structure grown on a bulk GaN substrate: (a) $1\times1\,\mu m^2$ scan; (b) $5\times5\,\mu m^2$ scan; both scans have a *z*-height scale of 5 nm.

3.1.2. Performance characteristics of mesa type rectifiers on GaN substrates

The homoepitaxial growth of GaN layers on lattice-matched GaN substrates have the potential to reduce threading dislocation densities significantly due to reduction of the thermal and lattice mismatch between the layers and the substrate compared to growth on conventional sapphire and SiC substrates. However, there have been only a few reports on GaN *p-i-n* rectifiers grown on GaN substrates. To date, power switching devices performing at or near the theoretical limits for GaN have not been reported. It is believed that the electrical performance of GaN high-power devices will improve with the reduction in the dislocation density as well as

with improve device design and processing techniques. As described in the previous section, we used the *n*-type bulk "free-standing" GaN substrates grown by HVPE (hydride vapor phase epitaxy) with a dislocation density of $<1\times10^{8}$ cm^{-2} ("LED quality" by the manufacturer's designation) for the rectifier structure growth. We need to point out that the dislocation density of the substrate used in the study is lower than GaN template grown on sapphire substrates (1×10^{8}~1×10^{9}cm^{-2}) but still higher than state-of-the-art bulk GaN substrates (5×10^{5}~5×10^{6}cm^{-2}).

After the epitaxial growth of *p-i-n* rectifiers on GaN substrates, the microscopic surface morphology was characterized by AFM. Figure 7 shows AFM images (using a *z*-height of 5 nm) exhibiting atomically smooth surfaces. The RMS roughness values are approximately 0.169 nm and 0.234 nm for a 1×1 μm^2 scan and a 5×5 μm^2 scan, respectively. As expected, the full-width-at-half-maximum (FWHM) line-widths of the GaN-epitaxial layer related peak from the X-ray rocking curve replicates the FWHM of GaN substrates.

The high-voltage reverse characteristics for rectifiers grown on a GaN substrate are shown in Figure 8(a). The reverse current density is $I_r \sim 0.1$ A/cm^2 at $V_r \sim -500$ V, with a blocking voltage of $V_r \sim -540$V. The forward *I-V* characteristics are shown in Figure 8(b). The forward voltage drop is ~4.4 V at a typical forward current density of 100 A/cm^2, with the maximum current density exceeding 1000 A/cm^2. The specific On-resistance is $R_{ON} \sim 3$ mΩ·cm^2. These values yield a figure-of-merit value for $(V_{RB})^2/R_{ON} = 97.2$ MW/cm^2 [7]. These values are close to the simulation results for this device structure using a commercial device simulator, which predict a breakdown voltage $V_r \sim -700$V and a forward voltage drop of 3.3V at a forward current density of 100 A/cm^2 [8]. Analysis of the forward *I-V* characteristics indicate a diode ideality factor of $n\sim2.59$ for device on SiC and $n\sim3$ for device for on GaN substrate a forward voltage ~3 V, as expected for recombination dominated transport in the space-charge region. Beyond a forward voltage ~3V, the current is limited by the device series resistance. A high forward voltage drop is expected for wide-bandgap materials, especially for direct-bandgap semiconductors like GaN that have extremely short carrier lifetimes relative to indirect-bandgap semiconductors like SiC [9].

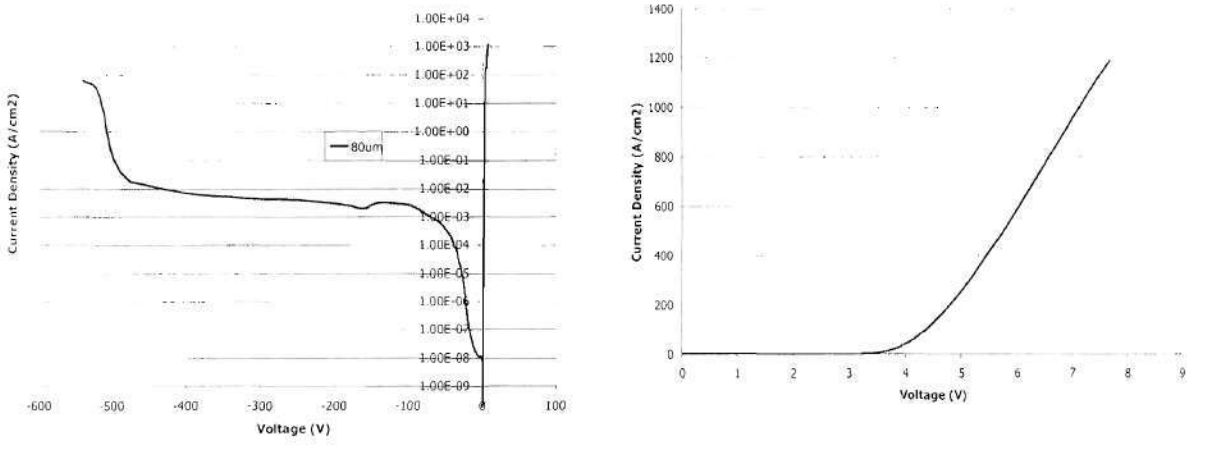

Figure 8: *I-V* characteristics of *p-i-n* rectifier on GaN substrate and (b) forward characteristics of *p-i-n* rectifier on GaN substrate.

3.2. GaN *p-i-n* Full Vertical Type Rectifiers

3.2.1. Full vertical structure on *n*-type SiC substrates

For the growth of GaN on a SiC substrate, AlN grown at high temperature has been shown to be a suitable buffer layer. This is because SiC-AlN has a relatively small *a*-axis lattice mismatch of approximately 1% [10], however, one of the problems of using undoped AlN as a buffer layer is that it is essentially an insulator having a large ionization activation energy of ~320 meV for Si donors [11] as well as a large energy bandgap of 6.2 eV. As a result, when a GaN-based device is grown on a SiC substrate with an AlN buffer layer, a back-side contact to the SiC substrate with a full-vertical device configuration can not be realized; hence, with a conventional AlN buffer layer and mesa structure, the excess leakage current through sidewall damage by deep dry etching is unavoidable. As one of the alternative approaches, a low Al-composition AlGaN (up to an Al-mole fraction ~0.15), which can be directly grown on SiC substrates with reasonably conductive characteristics has been studied; however, the phase separation with the fluctuation of Al content and three-dimensional GaN island morphology have been observed. The difference in the surface mobility between Al and Ga atoms on the growing surface which is one of the crucial parameters in AlGaN growth has also been published [12]. In this report, the demonstration of the growth and fabrication of GaN *p-i-n* rectifiers with a full-vertical geometry employing $Al_xGa_{1-x}N$:Si ($x = \sim 0.1$) as a conducting buffer layer is described.

The development of a full-vertical GaN *p-i-n* rectifier on a 6H *n*-type SiC substrate by employing a conducting $Al_xGa_{1-x}N$:Si ($x = \sim 0.1$) buffer layer scheme is reported. In this vertical configuration, the *n*-contact is made on the back-side of the SiC substrate using a Ni/Au metallization scheme. Epitaxial layers are grown similar to the conventional structure with the exception of using an $Al_xGa_{1-x}N$:Si nucleation layer. The conducting $Al_xGa_{1-x}N$:Si layer is found to provide excellent electrical properties while also acting as a good nucleation layer for subsequent GaN growth.

3.2.2. Conducting buffer layer development on *n*-type SiC substrates

To overcome the technological barriers associated with insulating AlN buffer layers, high-temperature grown AlGaN:Si layers were investigated to realize a full-vertical GaN *p-i-n* structure for rectifier applications. The layer is required to satisfy two conditions to serve as conducting buffer layer: (1) it needs to be vertically conducting through the buffer and substrate and (2) it should be effective as a buffer layer in terms of the crystalline and structural quality for the subsequent growth of epitaxial layers [13]. The Al mole fraction, x, of the AlGaN layer was measured to be approximately x~0.1, determined from photoluminescence and XRD. The carrier concentration in the $Al_xGa_{1-x}N$:Si ($x= \sim 0.1$) layer was estimated to be $n=3\times10^{18}$ cm^{-3}. The vertical transport characteristics of *n*-type $Al_xGa_{1-x}N$:Si ($x= \sim 0.1$) on a *n*-type SiC substrate were studied to determine the electrical properties. For this purpose, a metallization scheme using Ti/Al/Ti/Au on top of the *n*-AlGaN:Si and Ni/Au on the backside of the *n*-type SiC substrate was deposited by an electron-beam evaporator system. As shown in Figure 9, the structure demonstrated excellent current voltage characteristics between the *N-n* heterojunction with a 180 μm diameter circular mesas. A small kink was observed on forward bias condition and it is believed to originate from the heterostructure barrier between *N*-AlGaN and *n*-SiC junction due to the band-offset combined with Fermi level pinning effect by interface defect [14]. Another possibility to the origin of kink can be non-ideal ohmic contact behavior; however, the ohmic

behavior of the contact, especially for *n*-AlGaN, was verified by TLM (transmission line measurement) study. The surface morphology of a GaN *p-i-n* grown on an $Al_xGa_{1-x}N$:Si (x= ~ 0.1) conducting buffer layer was also characterized by AFM and it resulted in the smooth surface with the RMS roughness values of 0.44 nm and 0.63 nm for a 1×1 μm^2 scan and 5×5 μm^2 scan, respectively.

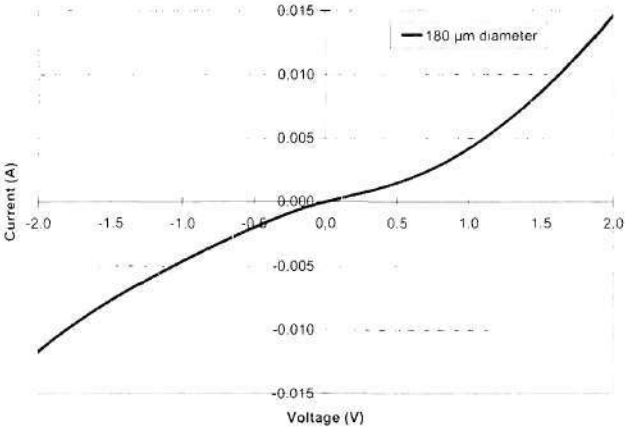

Figure 9: The vertical transport characteristics of $Al_{0.1}Ga_{0.9}N$:Si conducting buffer layer grown on an *n*-type 6H-SiC substrate.

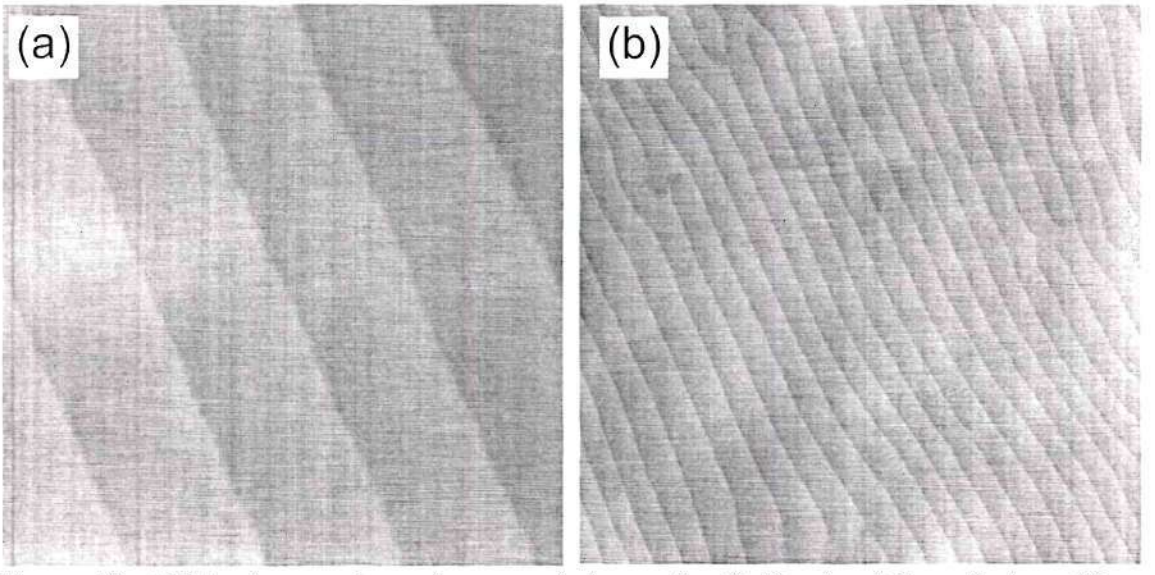

Figure 10: AFM microscopic surface morphology of a GaN *p-i-n* full-vertical rectifier structure on an *n*-AlGaN:Si conducting buffer layer grown on an *n*-type (0001) 6H-SiC substrate: (a) 1×1μm^2 scan (b) 5×5μm^2 scan with the *z*-height scale of 10 nm.

Examination with a Nomarski optical microscope confirmed the smooth surface for a full-vertical GaN *p-i-n* rectifier structure with $Al_xGa_{1-x}N$:Si (x = ~0.1) as a conducting buffer

layer. An $Al_xGa_{1-x}N$:Si (x = ~ 0.1) layer graded to GaN:Si layer was inserted as a strain relaxation layer underneath the *n*-type GaN. The microscopic surface morphology was characterized by AFM. Figure 10 shows AFM images (under the *z*-height of 10 nm) revealing atomically smooth surface with no visible nano-pits. RMS roughness values are approximately 0.22 nm and 0.26 nm for 1×1 μm^2 scan and 5×5 μm^2 scan, respectively. The crystalline quality of GaN epitaxial layers on a conducting buffer layer/SiC substrate for full-vertical structure was analyzed using a high-resolution X-ray diffractometer. The full-width-at-half-maximum (FWHM) line-widths of the GaN-related peaks were ~180 arc-sec. and ~320 arc-sec. for (002) and (102) scan respectively, which are comparable to those of GaN *p-i-n* rectifier structures employing a conventional AlN buffer layer on SiC substrates.

3.2.3. Performance characteristics of full vertical rectifiers on SiC substrates

The epitaxial structure for the rectifier is similar to that of the mesa device. It consists of, in the order of top to bottom layers, GaN:Mg^{++} contact layer, *p*-GaN:Mg, 2.5μm-thick unintentionally doped GaN, *n*-GaN:Si, AlGaN:Si conducting buffer layer. The schematic structural design of a full-vertical GaN *p-i-n* rectifier is illustrated in Figure 11(a). The energy-band diagram of the epitaxial structure for the device is also shown in Figure 11 (b). For the construction of energy-band diagram, a one-dimensional simulation [15] was applied to the GaN *p-i-n* structure. The intrinsic doping level of unintentionally doped *i*-GaN was assumed to be n~5×10^{16} cm^{-3} and spontaneous and piezoelectric polarization effect was not considered in the simulation.

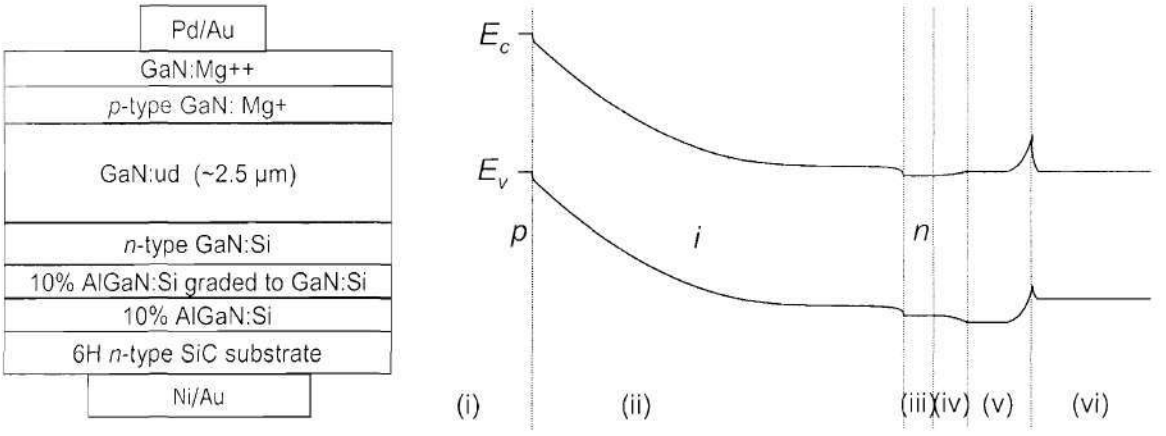

Figure 11: (a) Schematic structure of a full-vertical GaN *p-i-n* rectifier used in this work and (b) energy band diagram of the epitaxial structure in thermal equilibrium: (i) *p*-GaN:Mg, (ii) unintentionally doped *i*-GaN, (iii) *n*-GaN:Si, (iv) AlGaN-GaN grading, (v) AlGaN conducting buffer layer , and (vi) *n*-SiC substrate.

The top *p*-type contact was a circular pattern while the *n*-type contact covered most of backside of the SiC substrate. Two configurations of devices were compared: One does not have any current guiding scheme and the other has current guiding only in *p*-layer. To provide the current guiding in *p*-layer, the layer was shallow-etched by ICP etching and passivated by

SiO_2. Performance characteristics are compared. Both configurations show a low on-resistance of 7.5×10^{-3} $\Omega\cdot cm^2$. The reverse breakdown voltage for rectifiers without *p*-current guiding was over -330V, while one with *p*-current guiding was over -400V (Figure 12). The devices with *p*-current guiding exhibit much reduced reverse leakage current, indicating that the current guiding even in relatively thin *p*-layer facilitates the reduction of the reverse leakage current and improves the device performance characteristics.

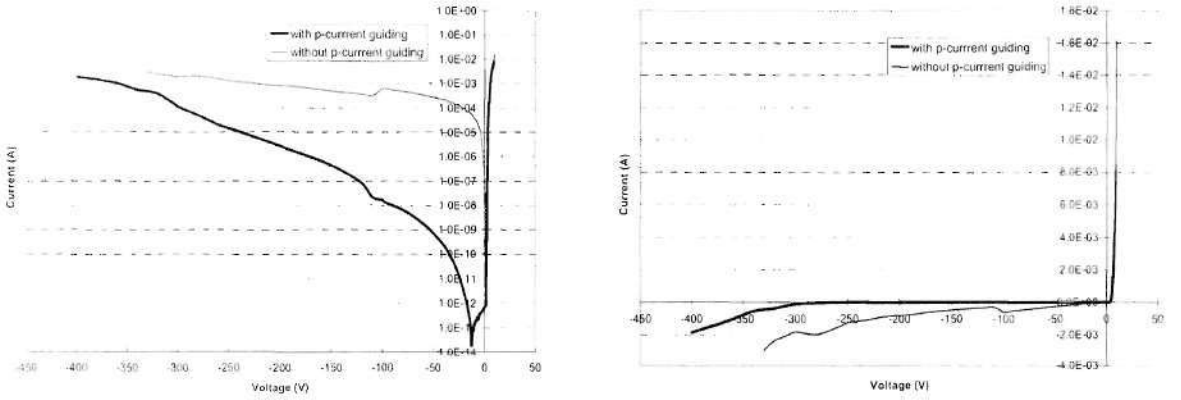

Figure 12: (a) Current-voltage characteristics of a full-vertical GaN *p-i-n* rectifier (log scale) (b) Current-voltage characteristics of a full-vertical *p-i-n* rectifier (linear scale).

4. Summary and Future Work

During the last year in the "rectifier task" of this program, we explored the GaN-based *p-i-n* rectifiers with mesa type and full vertical device geometry on SiC and GaN substrates. For mesa rectifiers grown on SiC substrates, we have achieved the blocking voltage of $V_r \sim$ -500 V and the specific On-resistance of R_{ON} ~2.3 m$\Omega\cdot cm^2$, which yield a figure-of-merit value for $(V_{RB})^2/R_{ON}$ = 108 MW/cm^2. For mesa rectifier grown on GaN substrate, the high-voltage reverse characteristics with a blocking voltage of $V_r \sim$ -540V and the specific On-resistance of $R_{ON} \sim 3$ m$\Omega\cdot cm^2$ were demonstrated. These values yield a figure-of-merit value for $(V_{RB})^2/R_{ON}$ = 97.2 MW/cm^2. These values are close to the simulation results for this device structure using a commercial device simulator, which predict a breakdown voltage V_r ~-700V and a forward voltage drop of 3.3V at a forward current density of 100 A/cm^2. Growth on lower-dislocation GaN substrates should help improve reverse breakdown characteristics. For full-vertical rectifiers on SiC substrates, conducting buffer layer with excellent electrical and structural properties was demonstrated. The reverse breakdown of a full-vertical GaN *p-i-n* rectifier with the relatively thin 2.5 μm-thick *i*-region was V_{BR} > -400 V with on-resistance of $R_{ON} = 7.5\times10^{-3}$ $\Omega\cdot cm^2$. The devices showed the breakdown voltage and leakage current dependence only with *p*-current guiding, indicating that the further current guiding should facilitate the reduction of the reverse leakage current and improves the device performance characteristics.

We note that all of the GaN *p-i-n* rectifier devices described above showed a breakdown mechanism that was "catastrophic" and was not reversible. The breakdown occurred on the

edges of the device mesa or somewhere in the mesa due to dislocations and microplasmas. However, true "avalanche" breakdown has recently been observed by Dupuis' Group for GaN *p-i-n* homoepitaxial devices (grown on bulk GaN substrates with low dislocation density of the order of 10^6 cm^{-2} in contrast to the GaN substrate for rectifier structure growth in the section 3.1.2. having dislocation density of the order of 10^7 cm^{-2}) with thinner "*i*-layers" (t~0.25 μm) giving a lower true avalanche reverse breakdown voltage of ~-85V (see Figure 13).[16] This breakdown mechanism is due to avalanche generation of carriers in reverse bias as has been confirmed by variable-temperature breakdown measurements and light-response vs. reverse-bias testing. The reverse-bias saturation current is extremely low and is less than $1x10^{-12}$ A over the reverse bias voltage range $0 < |V_R| < 65$ V. These devices can be operated into avalanche over 40 times with no adverse effects on the operating characteristics. This work suggests that true high-voltage rectifiers can be obtained from GaN *p-i-n* devices grown on "low-dislocation density" bulk GaN substrates if the required "guard-ring" structures can be developed. Future work in this area will concentrate on improvements in this design and the use of improved GaN substrates. We believe that these advances will lead to the development of GaN-based *p-i-n* rectifiers having a reverse-bias avalanche breakdown voltage >1,000 V and a near-theoretical low on-resistance.

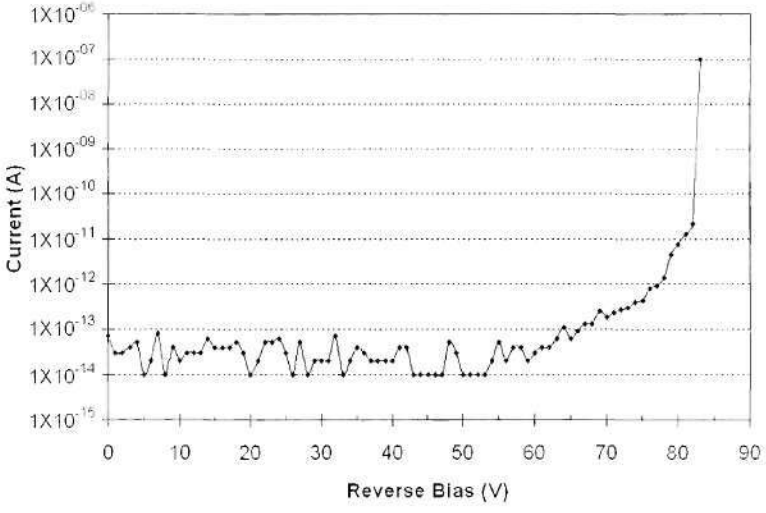

Figure 13: Reverse-bias dark-current characteristics of a GaN *p-i-n* structure with *i*-layer thickness of 0.25 μm grown on a GaN bulk substrate having a circular mesa of 30 μm diameter, showing a low dark current and current density of 2×10^{-11} A and 3.5×10^{-6} A/cm^2 respectively, at a reverse bias ~82 V.

References

[1] S. Nakamura, and G. Fasol, *The Blue Laser Diode,* Springer-Verlag, Berlin,1997.
[2] Irokawa, Y., Luo, B., Kang, B.S., Kim, J., Laroche, J.R., Ren, F., Baik, K.H., Pearton, S.J., Pan, C.-C., Chen, G.-T., Chyi, J.-I., Park, S.S., Park, Y.J.: '2.6A, 0.69MWcm^{-2} single chip bulk GaN p-i-n rectifier', *Sol.-Stat. Elec.,* 2004, **48**, pp. 359-361
[3] Irokawa, Kim, J., Ren, F., Baik, K.H., Gila, B.P., Abernathy, C.R., Pearton, S.J., Pan, C.-C., Chen, G.-T., Chyi, J-.I., Park, S.S., "Si^{+} ion implanted MPS bulk GaN diodes", *Sol.-Stat. Elec.,* 2004, **48**, pp. 827-830
[4] The reactor is manufactured by Thomas Swan Scientific Equipment Ltd., Cambridge, UK
[5] Obtained from Epichem Inc., Haverhill, MA
[6] The substrates were provided by Limilog, Vallauris, France; for more information including substrate specification, "http://www.lumilog.com"
[7] J. B. Limb, D. Yoo, J.-H. Ryou, W. Lee, S.-C. Shen, and R. D. Dupuis, "High voltage operation of GaN *p-i-n* rectifiers grown on freestanding GaN substrates," *Electron. Lett.* (submitted for publication).
[8] B. S. Shelton, T. G. Zhu, D. J. H. Lambert, and R. D. Dupuis, "Simulation of the Electrical Characteristics of High-Voltage Mesa and Planar GaN Schottky and PIN Rectifier", *IEEE Trans. Electron. Dev.*, 2001, **45**, pp. 1498-1502
[9] Chernyak, L., Osinsky, A., Temkin, H., Yang, J.W., Chen, Q., and Khan, M.A., 'Electron Beam Induced Current Measurements of Minority Carrier Diffusion Length in Gallium Nitride', *Appl. Phys. Lett.,* 1996, **69**, pp.2531-2533
[10] T. Weeks Jr., M. Bremser, K. Ailey, E. Carlson, W. Perry, and R. Davis, *Appl. Phys. Lett.* **67**, 401 (1995).
[11] R. Zeisel, M. W. Bayerl, S. T. B. Goennenwein, R. Dimitrov, O. Ambacher, M. S. Brandt, and M. Stutzmann, *Phys. Rev.* **B 61**, R16283 (2000).
[12] S. Heikman, S. Keller, S. DenBaars, U. Mishra, F. Bertram, and J. Christen, *Jpn. J. Appl. Phys.* **42**, 6276 (2003).
[13] D. Yoo, J. Limb, J. H. Ryou, W. Lee, and R. D. Dupuis, "Full-vertical GaN *p-i-n* rectifier employing AlGaN:Si conducting buffer layer on *n*-SiC substrate," *Appl. Phys. Lett.* **88**, 193503 (2006).
[14] Y. Huang, X. D. Chen, S. Fung, C. D. Beling, C. C. Ling, X. Q. Dai, and M. H. Xie, *Appl. Phys. Lett.* **86**, 122102 (2005).
[15] 1-D Poisson by Prof. Gregory Snider with the University of Notre Dame was used.
[16] J. B. Limb, D. Yoo, J. H. Ryou, W. Lee, S. C. Shen, R. D. Dupuis, M. L. Reed, C. J. Collins, M. Wraback, D. Hanser, E. Preble, N. M. Williams, and K. Evans, "GaN Ultraviolet Avalanche Photodiodes with Optical Gain Greater Than 1,000 Grown on GaN Substrates by Metalorganic Chemical Vapor Deposition," Appl. Phys. Lett., accepted for publication (2006).